Journal of Geophysical Research: Atmospheres

RESEARCH ARTICLE
10.1029/2018JD028583

Mapping the Lateral Development of Lightning Flashes From Orbit

Michael Peterson[1], **Scott Rudlosky**[2], **and Wiebke Deierling**[3,4]

[1]Cooperative Institute for Climate and Satellites-Maryland, Earth System Science Interdisciplinary Center, University of Maryland, College Park, MD, USA, [2]NOAA/NESDIS/STAR, College Park, MD, USA, [3]Department of Aerospace Engineering Sciences, University of Colorado Boulder, Boulder, CO, USA, [4]National Center for Atmospheric Research, Boulder, CO, USA

Key Points:
- Lightning imagers provide a 2-D composite view of the horizontal development of lightning flashes
- Flash properties typically describe the most radiant group while group-level data document flash evolution and structure
- Flash propagation encompasses velocity scales of 10^4 and 10^6 m/s, consistent with leader development

Supporting Information:
- Supporting Information S1

Correspondence to:
M. Peterson,
michaeljp24@gmail.com

Citation:
Peterson, M., Rudlosky, S., & Deierling, W. (2018). Mapping the lateral development of lightning flashes from orbit. *Journal of Geophysical Research: Atmospheres*, *123*, 9674–9687. https://doi.org/10.1029/2018JD028583

Received 26 FEB 2018
Accepted 13 AUG 2018
Accepted article online 27 AUG 2018
Published online 12 SEP 2018

Abstract Optical lightning measurements from the Lightning Imaging Sensor (LIS) are used to map the lateral development of lightning flashes and produce statistics that describe their motion through the electrified cloud. This is accomplished by monitoring the frame-by-frame (group-level) evolution of the optical signals produced during each flash. While the optical flash properties recorded by LIS gravitate towards the most exceptional optical signals produced during the flash, group-level data describe the evolution and lateral development of the flash resulting from physical lightning process that emits enough light out of the top of the cloud to be detected from orbit. The groups that comprise LIS flashes constitute examples of complex lateral flash structure that can extend 80 km in length with dozens to hundreds of visible branches. The lateral development of individual flashes is described in terms of its speed and direction of motion, whether the development extends the overall length of the flash or reilluminates an existing segment, and whether it is directed inbound or outbound with respect to the origin. Sixty-five percent of propagating groups are directed outbound from the origin, 22% extend the length of the flash, and 3–5% reilluminate an existing branch. LIS flashes are commonly oriented from east to west and develop at speeds ranging from 10^4 to 10^6 m/s, consistent with large-scale leader development. These results provide evidence that lightning imagers may be used in conjunction with Lightning Mapping Array systems to document physical lightning phenomena across global domains.

Plain Language Summary Lightning imagers on satellites measure all types of lightning flashes with a high probability of detection. They can also be used to document the evolution of individual lightning flashes and examine their lateral structure. This study uses Lightning Imaging Sensor measurements to identify what level of spatial and temporal development that can be detected by lightning imagers. We find that orbital lightning sensors observe lateral flash development that is consistent with physical lightning processes. These results suggest that lightning imagers can make viable lightning mappers that can be used to examine lightning physics in flashes across the globe. This is particularly important for remote regions such as the open ocean where flash development is not observed by other means.

1. Introduction

Lightning is a transient high-current atmospheric phenomenon that radiates across the electromagnetic spectrum (Uman, 1987). Lightning produces multiple optical and radio frequency pulses as the discharge extends or retraces the lightning channel. Localizing these signals to geographical coordinates makes it possible to map the development of a lightning flash in space and time. Radio frequency lightning mapping techniques, in particular, have changed the way the community views lightning. The American Meteorological Society Glossary of Meteorology has traditionally defined a lightning discharge as "a series of electrical processes taking place within one second." However, lightning flashes have been detected by regional Lightning Mapping Array (LMA; Rison et al., 1999) networks that last many seconds and extend over hundreds of kilometers. The World Meteorology Organization recently recognized two LMA flashes with the longest reported extent at 321 km, and the longest reported duration at 7.74 s (Lang et al., 2017).

The physics and underlying meteorology in these extreme flashes differ significantly from the standard thunderstorm models that produce typical cloud-to-ground (CG) and intracloud flashes. Flashes that extend hundreds of kilometers are not solely under the influence of separated pockets of charge within a single convective cell. Indeed, both extreme flashes in Lang et al. (2017) leave the convective core of

the parent thunderstorm and propagate laterally deep into the stratiform region. Horizontal propagation is guided by potential wells, or maxima and minima in the local electric field profile (Coleman et al., 2003). Unlike the charge structures of convective cells that can be described using a vertical dipole or tripole model (Williams et al., 1989), stratiform clouds develop a series of horizontally expansive stacked charge layers of alternating polarity (Lang et al., 2004; Marshall & Rust, 1993; Marshall et al., 2009; Stolzenburg et al., 1994). These layers result from a combination of the advection of charged ice particles from the convective core and in situ charging processes within the stratiform region (Ely et al., 2008; Lang & Rutledge, 2008; Rutledge & MacGorman, 1988; Schuur & Rutledge, 2000). Significant lateral flash development is thus a consequence of thunderstorm dynamics and may be used as an indicator of convective organization and maturity.

Optical lightning measurements provide a different perspective on flash structure than RF networks. Leader development has been documented using high-speed camera imagery since the 1930s (Schonland et al., 1935). Modern ground-based camera systems can detect fine structures associated with negative step leader formation such as space stems and corona streamer filaments (Hill et al., 2011). Detailed high frame rate optical measurements of the lightning channel are possible so long as the flash is not obscured by clouds or rainfall between the lightning strike and the observer.

Satellite lightning imagers, in contrast, detect lightning by measuring changes in cloud top radiance due to lightning activity. Because they measure at the 7774 Å oxygen emission line, they can detect total lightning at all times of day with a detection efficiency that ranges from ~69% at noon to ~88% at night (Cecil et al., 2014). Three generations of lightning imagers have been deployed before 2018: the Optical Transient Detector (Boccippio et al., 2000) on the MicroLab-1 satellite (1995–2000), the Lightning Imaging Sensor (LIS; Blakeslee et al., 2014; Christian et al., 2000) on both the Tropical Rainfall Measuring Mission (TRMM) satellite (1997–2015) and the International Space Station (2017 to present), and the Geostationary Lightning Mapper (GLM; Goodman et al., 2013) on the Geostationary Operational Environmental Satellite 16-series (2016 to present).

Lightning imagers map the evolution of optical energy produced by lightning in space and time at a nominal 500 frames per second. The primary motivations for examining the frame-by-frame evolution of individual flashes have been to validate independent lightning measurements (Rudlosky et al., 2017) and to identify important components of the flash such as the return stroke (Koshak, 2010) or continuing currents (Bitzer, 2017). Changes in the extent, position, and radiance of the optical signals are indicative of such physical lightning processes, but these signals are modified by scattering in the cloud medium (Peterson, Deierling, et al., 2017; Thomson & Krider, 1982). Thomas et al. (2000) found an excellent spatiotemporal agreement between LIS observations and Oklahoma LMA sources for flashes that extended into the upper part of a storm. Scattering within the cloud through a large optical depth limited detection of the lowest extents of CG discharges, particularly during their earliest development.

Cloud scattering effects provide a unique challenge to the process of mapping lightning flashes from above with optical sensors. Not only will weak optical signals at cloud top that fall below the instrument background threshold be excluded but also particularly radiant pulses can illuminate a large area of cloud far beyond the extent of the flash before or after that point. The largest of these occur near the edges of convective cloud features where the optical energy escaping the side of the cloud can illuminate the top of a lower cloud deck (Peterson, Rudlosky, et al., 2017). When mapping optical flashes with optical sensors, it is necessary to distinguish between flash developments that result from physical lightning processes—that is, strokes, K-changes, and leader development—and those that occur due to scattering across the cloud scene. Only the former will provide useful insights into the scale and speed of flash development.

Though lightning imagers are not able to provide the level of detail and three-dimensional accuracy of regional line-of-sight LMA systems, the global-scale coverage afforded by orbital platforms makes their lightning flash extent maps valuable for lightning hazard applications as well as physical lightning research. The vertically integrated two-dimensional LIS and GLM view of lateral flash structure is sufficient for identifying lightning that occurs outside of the convective core (Peterson & Liu, 2011) that propagates over significant horizontal distances—such as the extreme flash cases from Lang et al. (2017)—or that has a complex optical structure (Peterson & Liu, 2013; Peterson, Rudlosky, et al., 2017). Satellite lightning platforms such as International Space Station-LIS and GLM provide a means of documenting the evolution of lightning

offshore—for example, in the eastern Mediterranean, the Pacific Ocean east of Japan, or in hurricanes and tropical storms—or in land-based regions that lack LMA coverage such as the Congo Basin in Africa.

The present study examines the use of frame-by-frame optical lightning measurements to map the lateral development of lightning flashes from orbit. LIS measurements are used to establish statistics for the horizontal scale and complexity of optical flashes, the speed at which flashes develop laterally, and their orientation and direction of motion.

2. Data and Methodology

2.1. The Composition of Optical Flashes

This study leverages the LIS science data set hosted at the Global Hydrology Resource Center to create a database that quantifies flash evolution with time. The LIS grouping algorithms described in Christian et al. (2000) and Mach et al. (2007) cluster optical lightning signals into features that describe lightning on a number of scales. The smallest optical lightning feature is the LIS "event." An event is a single LIS pixel at a given point in time that exceeds the dynamic background radiance threshold. Contiguous events in the same 2-ms LIS frame are clustered into "groups" that describe the portions of the LIS field of view that are illuminated by lightning. Groups that occur close to one another in time and space are then clustered into "flashes" and nearby flashes are clustered into "area" features that approximate thunderstorms.

The LIS flash features are sufficient for applications that are concerned with whether lightning occurred or computing the total flash rate, but the LIS groups and events that comprise each flash are needed to describe the evolutions of individual flashes. Figure 1 shows the components of an example propagating LIS flash. The plan view of the events (large boxes) and group centroids (small boxes) in the flash is shown in the center of the figure (Figure 1c) overlaid on a plot of TRMM Visible and Infrared Scanner (VIRS) infrared brightness temperatures. Events and groups are color coded by group number (dark gray: first group; white: last group). Group centroids are connected to the nearest preceding group to form a skeleton image of the group-level structure. Cross sections by longitude and latitude are shown above and to the right of the plan view, respectively. The longitude and latitude extent of the LIS groups over the course of the flash is shown in Figures 1b and 1d. TRMM Precipitation Radar (PR) cross sections through the center of Figure 1c are also shown in Figures 1a and 1e. Finally, a group area time series is shown below the plan view in Figure 1f.

The blue shaded regions in Figure 1f denote clusters of LIS groups that occur over multiple frames. We define these features as LIS "series," and they are meant to describe distinct optical pulses that are separated by "dark" periods with no groups detected. These features result from physical lightning processes such as propagation (Peterson, Deierling, et al., 2017) or continuing current (Bitzer, 2017). A series feature is defined as any collection of groups within the same flash separated in time by no more than 1 LIS frame. A LIS series may contain a single LIS group (a "singleton" series) or all groups in the flash. For the example in Figure 1, 28 multiple-group series are noted with durations that range from 4 to 65 ms.

2.2. Measuring Flash Extent and Complexity

Figure 1 depicts a stratiform flash that began in the southeast portion of its footprint near the edge of the convective core (dashed area in Figure 1c). It propagated to the west-by-northwest 83 km into the stratiform region over the course of 2.2 s. The groups branched out in multiple directions as the flash evolved. A first glance reveals at least five distinct branches in the group-level structure. The exact number of evident branches depends on how the group-level skeleton is constructed and which types and scales of lateral motion should be counted as a "branch."

We automate flash skeleton creation and branch counting to enable statistical analyses of flash extent and complexity. Figure 2 isolates the flash skeleton for the case in Figure 1 (thin lines in Figure 1c). "Branches" are distinguished as uninterrupted line segments between junctions in the skeleton that are at least 1 LIS pixel in size (~5 km). Skeleton branches in Figure 2 are color coded and numbered. There are 102 in total with most consisting of 1–2 groups attempting to break away from the main channel (i.e., 4, 8, 17, 55, and 63). When these junctions occur, two new branches are defined—one for the breakout branch and one for the continuation of the existing channel. Multiple failed branches occurring close to one another can also cause a single valid branch to be split in two, increasing the branch count. Thus, while the branch feature counts

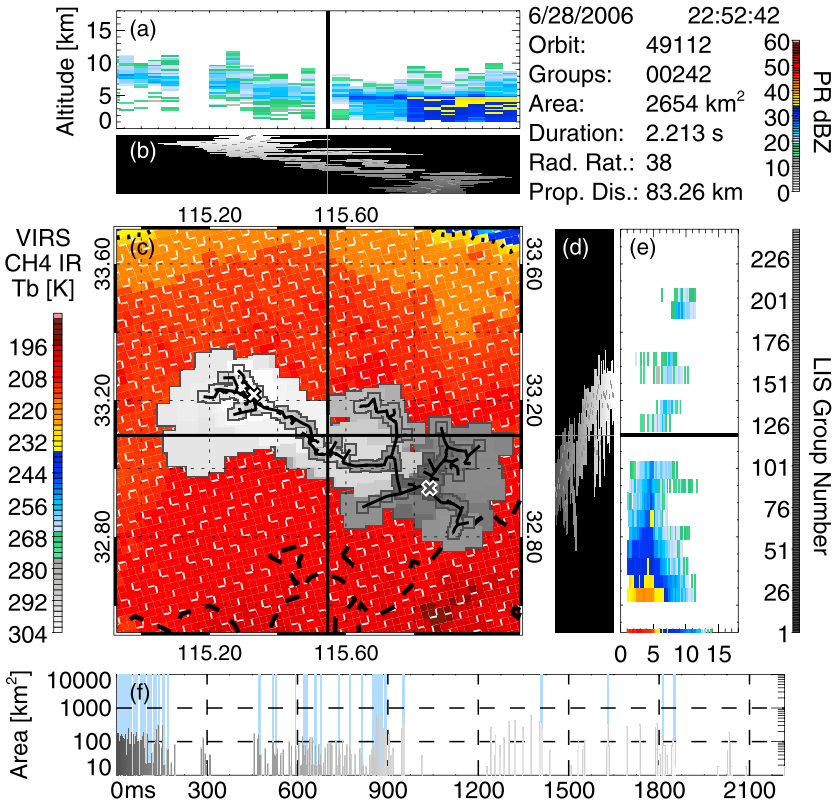

Figure 1. An example propagating LIS flash. LIS events (large pixels) and group centroids (small boxes) are color coded in a grayscale by LIS group number ordered temporally from first light (gray) to last (white). Centroid locations of first and last light shown as X's. (a) PR reflectivity longitude-altitude cross section. (b) Longitude extent of LIS groups as a function of sequential group number. (c) Plan view on top of Visible and Infrared Scanner (VIRS) CH4 10.8 μm brightness temperatures. (d) Latitude extent of LIS groups as a function of sequential group number. (e) TRMM PR reflectivity latitude-altitude cross section. (f) The timing of LIS groups (same grayscale as before) and series (shaded blue), and the temporal evolution of LIS group area. LIS = Lightning Imaging Sensor; PR = Precipitation Radar.

shown in Figure 2 are useful for identifying flashes with complex group-level structures, they are notably higher than the number obtained by counting manually using human intuition.

The flash skeletons offer an alternative to the LIS-illuminated cloud footprints for estimating the extent of a given flash. The flash footprint responds to lateral flash development as well as radiative transfer in the surrounding cloud. A large flash with a footprint area in the thousands of square kilometers may be an example of a propagating flash like the case in Figure 1, or it may be a radiant superbolt with little motion between groups. Examples of each case are identified and discussed in Peterson, Rudlosky, and Deierling (2017). The flash skeleton, by contrast, tracks lateral motions between groups regardless of radiance. The size of the skeleton can be described in terms of the maximum separation of groups, as in Peterson, Deierling, et al. (2017), the total length of all skeleton branches (total propagation distance) or the area of the convex hull (CHULL) around the skeleton (white line in Figure 2). Flash footprint and skeleton areas are used to calculate characteristic length scales reported in kilometers. The characteristic length (or characteristic diameter) is defined as the distance across a disk with the same area as the feature in question, while the characteristic radius is half of the characteristic length.

2.3. Measuring and Classifying Motion Between Groups

Calculating the speed of flash development requires knowledge of the distance between two points along the lightning channel and the amount of time between the observations. These points do not have to be from the previous group as long as the origin point remains constant. van der Velde and Montanyà (2013) calculate leader propagation speeds by plotting the displacement and time of LMA sources from the

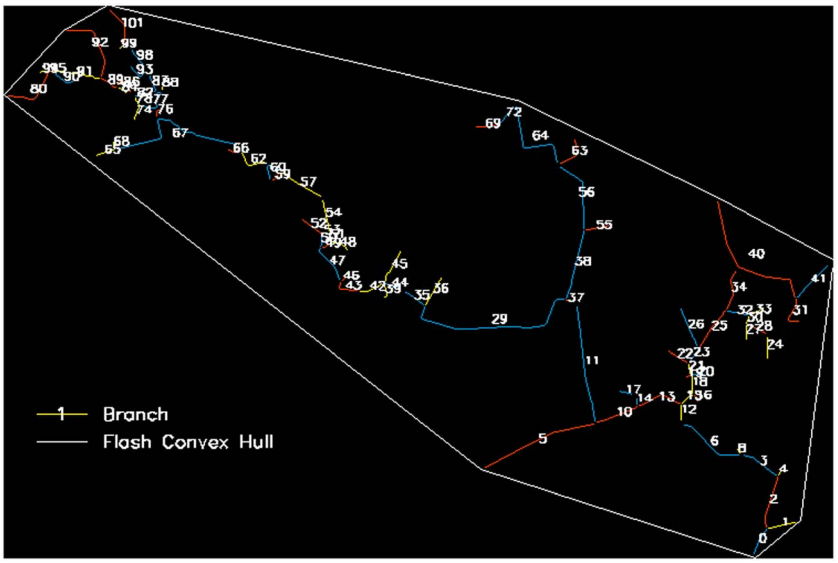

Figure 2. Skeleton image of the group centroids in the flash from Figure 1. Branches along the skeleton are color coded and numbered. A convex hull is drawn that bounds the groups in the flash skeleton.

latitude and longitude of a detected CG stroke and then fitting lines to clusters of sources that are assumed to represent distinct channels. Figure 3 applies a similar approach to the LIS group-level data for the flash in Figure 1, using the first light centroid location as the reference point for the origin of the plot. As in van der Velde and Montanyà (2013), many groups (circle symbols) cluster along linear features with average speeds of 1.8×10^5 and 1.1×10^5 m/s, well within the expected range of leader development, and on the same scale as the values given in the LMA study.

There are two key limitations with LIS compared to the LMA analysis in van der Velde and Montanyà (2013). The first is that optical sensors like LIS cannot report the polarity of leader development. This information may be inferred through data fusion with radio frequency observations, however. Second, the comparably low frame rates of satellite instruments make it difficult to resolve the fastest developing leaders. Leader development at 10^7 m/s over a distance of 20 km would take place in 2 ms and thus be contained within a single LIS group.

This linear clustering approach is not well suited for an automated analysis of flash velocities because it cannot account for radial motion. Rather, it only considers the displacement of points from the origin and thus often leads to clustering of points in different branches. The skeleton from Figure 2 is plotted in Figure 3 as lines connecting adjoining groups. The two prominent yellow lines that result in the speed estimates above designate branch development that extends the length of the flash. "Extending groups" account for the majority of groups in this flash, but groups along branches that do not extend the flash (gray lines) can be noted to the immediate right of the green lines in Figure 3. Most of these branches are nearly horizontal because they are oriented radially and terminate nearly as far from the flash origin as they begin. If these connecting lines were not drawn, then the clusters of groups at ~800 ms, from 1,200–1,400 ms or from 1,800–1,900 ms, might be automatically grouped into a leader.

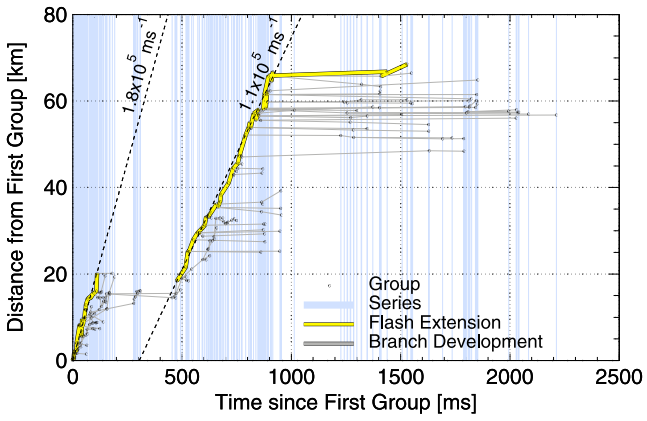

Figure 3. The time-distance distribution of groups in the example flash from Figures 1 and 2. The point of reference for the origin is the centroid of the first group in the flash. Groups are connected according to the skeleton from Figure 2. Groups that extend the flash length are marked in yellow. Series are shaded in blue.

To avoid this automation issue, we base our measurement of propagation speed on the distance and reported time between adjoining groups in the flash skeleton (Figure 2) rather than clusters in the time-distance plots. We carefully consider which types of groups should be used to make speed estimates. A notable aspect of LIS flashes is that their durations are mostly "dark" with groups dispersed sporadically throughout (i.e., Figure 1f). LIS cannot detect groups when the current flowing through the channel is

too low or there is a large optical depth of cloud between the emission source and the satellite. Moreover, on the distance side of the speed calculation, spacecraft motion and scattering in the cloud add uncertainty to the actual separation between points along the channel. These factors result in a large number of random motions at slow speeds ($<<10^5$ m/s) that add a low bias to the statistics. To address this, we only consider speeds computed using groups in the same series to ensure that distance measurements are based on a prolonged optical pulse.

The flash skeleton is also used to classify the nature of lateral flash development. As in Figure 3, we identify groups that extend the length of the flash and use the first light centroid location to define whether group motions are directed inbound or outbound. The orientation of the flash is determined using the major axis of the flash footprint (i.e., Figure 1c) while the overall direction of flash motion is approximated as the orientation of the flash skeleton CHULL (i.e., Figure 2). Finally, groups that occur at locations along an existing branch are classified as "reilluminating."

2.4. A LIS Flash Evolution Database

Metrics describing LIS flashes and groups are combined into a database that preserves the clustering hierarchy on a two-dimensional grid (flash number × group number). The database is built in this way to facilitate access between parameters that describe flashes overall (i.e., footprint area, propagation distance, and radiance) and detailed group-level metrics (i.e., group latitude, group longitude, time since first light, distance from previous group in branch, and branch reillumination flag). This database is built to test prototypes for LIS and GLM metrics that may eventually be useful as operational products. It contains a total of one million flashes from randomly selected TRMM orbits between 1998 and 2014. Series properties (count, duration, footprint area, etc.) are defined in a separate database and linked to the flash and group database through series identification parameters. Algorithmic formulations for all parameters in the flash evolutions database are provided in the supporting information Tables S1–S5.

3. Results

3.1. LIS Measurements of Optical Flash Extent and Complexity

Multiple methods exist to measure the lateral extent of an optical lightning flash. The standard flash size metric in the LIS science data set is the flash or group footprint area, which denotes the size of the cloud region illuminated by lightning. Because the footprint area and characteristic footprint diameter metrics describe the size of the cloud illuminated by the flash, they depend on the structure and energetics of the discharge as well as the geometry and scattering properties of the surrounding cloud medium. This sensitivity to the cloud scene made the flash footprint ideal for constructing LIS illuminated cloud features in Peterson, Deierling, et al. (2017) to examine connections between flash energetics and morphology and the microphysics of the cloud medium. For example, that study showed oceanic flashes to be more energetic than land-based flashes even when they occur at the same time of day and in similar types of clouds.

Radio measurements of flash length (Lang et al., 2017) or flash extent density (Bruning & MacGorman, 2013) are not entirely comparable with LIS flash footprints because the cloud has a negligible influence on the signals detected by radio receivers on the ground. With optical systems, some emitted energy will inevitably be scattered away from the receiver, and the signals that do arrive will be diluted across a sizable area. For lightning imagers to be used to map the lateral flash extents, a metric that is minimally sensitive to cloud scattering must be found.

The flash skeleton may fill this role. Figure 4a compares the average separation of events with the average separation of groups, CHULL characteristic length, and total propagation distance of all branches in the flash skeleton as a function of flash footprint length scale. The characteristic length of the flash footprint correlates primarily with the peak radiant energy of the flash. Energetic optical emissions scatter more photons through the cloud and push the radiance of more distant pixels above the background threshold for LIS, resulting in a large group footprint. Since most LIS flashes are comprised of many small and dim groups and a small number of highly radiant groups, these energetic groups often determine the optical footprint of the flash as well. The maximum separation of events increases monotonically with flash characteristic length since both parameters are based on event pixels. However, these measures do not match one-to-one. The maximum separation of events is calculated as the distance between pixel centers and can be zero for flashes that consist of a

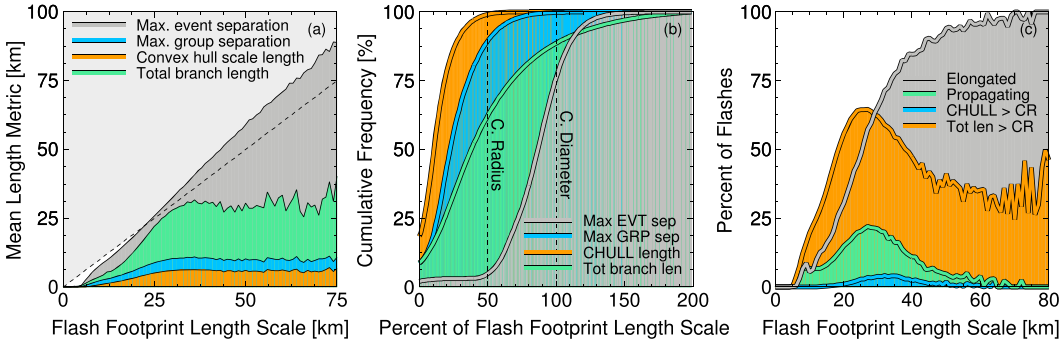

Figure 4. (a) Mean measurements of flash extent as a function of flash footprint length scale. (b) Cumulative distributions of flash extent as a percentage of flash footprint length scale. Characteristic radius and characteristic diameter thresholds are marked. (c) Fractions of flashes of a given footprint length scale that are classified as "propagating" or "elongated" or that have convex hulls or total branch lengths greater than the characteristic radius of the flash footprint. CHULL = convex hull; CR = characteristic radii.

single unique pixel. For a collection of perfectly circular flashes of varying sizes, the maximum event separations should be one pixel smaller than the characteristic footprint diameters because only the latter considers whole pixels in its formulation. This can be noted for flashes with characteristic lengths between 10 and 15 km across, where the average event separation lags behind the flash footprint characteristic length by ~5 km, the nominal pixel size of LIS. However, the event separation for larger flashes begins to outpace the diameter of the equivalent circular flash, and flashes that illuminate the largest cloud areas become increasingly elongated. The average flash with a 50-km characteristic diameter, for example, is measured at 66 km across for an elongation factor of 130%.

Peterson, Deierling, et al. (2017) and Peterson, Rudlosky, et al. (2017) identified cases that explain why large flashes often take on an elongated appearance. Some flashes, like the case in Figure 1 and the LMA extremes from Lang et al. (2017), are propagating flashes that move from one cloud region into another over time. The groups that comprise these flashes are generally small and relatively dim. The set of pixels that make up the later groups in the flash are often completely different from the set of pixels illuminated at first light. In flashes whose footprints are defined by dim cloud pulses, the events do not extend far beyond the flash skeleton or CHULL. Figures 1b–1d illustrate all of these aspects.

Many large elongated flashes are not examples of propagating flashes, however. A second species of enormous flash has CHULLs that are confined to a small portion of the overall flash footprint. Notable examples of these flashes with relatively stationary groups for their footprint size include the extreme area lightning flash from Peterson and Liu (2013), and the top LIS "superbolts" and flashes with the largest event separations from Peterson, Rudlosky, et al. (2017). They typically occur near the edge of the cold cloud with a majority of their pixels illuminating either anvil cloud with no radar echoes near the surface or lower clouds adjacent to the convective cell that initiated the flash.

Anvil flashes near the cloud edge owe their elongated footprints to the distribution of clouds across the scene. Radiance will only be scattered towards the satellite where clouds exist to direct it upwards. Picture a circular connective cell surrounded by a ring of lower boundary clouds. The footprint of a flash at the edge of the convective feature can only extend radially outward as far as the boundary cloud edge and is generally blocked by optically thick cloud mass in the inward radial direction. As a result, then the flash footprint will be significantly wider (tangentially) than it is long (radially). The top LIS flash in terms of event separation from Figure 4 in Peterson, Rudlosky, et al. (2017) shows this exact case where the flash footprint even curves around the edge of the convective feature.

Peterson, Deierling, et al. (2017) distinguished propagating flashes from other large elongated flashes by comparing the maximum group separation in the flash skeleton with the characteristic footprint length. Maximum group separation is defined as the largest distance between groups in a given flash. Flashes whose group separations accounted for at least the characteristic radius of the flash footprint were identified as "propagating." In contrast to the event-based measures of flash extent, measures of the size of the flash

skeleton in Figure 4a only increase with footprint area until ~30 km and then remain static as the flash footprint continues to grow. The pause in the growth of the group-level structure provides evidence that the flash skeleton is largely insensitive to radiative transfer effects and meets our needs for optical flash extent mapping.

While Figure 4a compares the length scales of different flashes, Figure 4b compares the different event- and group-based measures of flash extent to the footprint area of the same flash. Cumulative distributions are shown for the maximum separation of events, maximum separation of groups, CHULL characteristic length, and total length of all branches in the skeleton as a percentage of the flash footprint characteristic length. CHULL characteristic diameters and maximum group separations account for the smallest fractions of the footprint length scale. CHULLs are undefined for 19% of flashes for having less than the three unique group centroid locations required to bound a finite area. Similarly, the maximum group separation is undefined for 9% of flashes for having less than two unique group centroids. The median CHULL length scale accounts for 10% of the flash footprint length scale, while the median group separation accounts for 21% of the flash characteristic length. Peterson, Deierling, et al. (2017) would consider 11% of flashes in this sample "propagating" for having maximum group separations longer than the characteristic radius of the flash footprint (an x value of 50% in Figure 4b). The total propagation distance for all branches in this sample of propagating flashes, however, is a factor of 2 greater than the maximum group separation and can reach a length that is twice the characteristic diameter of the flash footprint on the extreme end of the distribution.

Figure 4c illustrates the fractions of LIS flashes that are considered elongated (maximum event separation $>$ characteristic diameter of the flash footprint) or propagating (maximum group separation $>$ characteristic radius of the flash footprint) in Peterson, Deierling, et al. (2017) as a function of flash footprint size. Also shown are curves for flashes with skeleton CHULL characteristic radii greater than the flash footprint characteristic radii (CHULL $>$ CR) and flashes with total skeleton branch lengths greater than the flash footprint characteristic radii (tot. len. $>$ CR). As in Figure 4a, the fraction of elongated flashes increases with footprint size. The fractions of propagating flashes and the two new categories (tot. len. $>$ CR and CHULL $>$ CR), however, peak between 25 and 30 km and account for $<$40% (tot. len. $>$ CR) or $<$10% (propagating, CHULL $>$ CR) of all flashes with characteristic lengths $>$30 km.

Histograms and cumulative distributions of the skeleton-derived flash length scales in Figure 4 and the total number of branches per flash are shown in Figure 5. Separate distributions are included for all LIS flashes and propagating LIS flashes that, by extension, will also have large CHULLs and total branch lengths. The histograms in Figure 5a span a range from 100 m to 150 km that includes the top 80% of CHULL scale lengths, the top 91% of maximum group separations, and the top 98% of total branch lengths. If the sample is limited to only propagating cases where the motion between groups accounts for a significant fraction of the footprint size, as in Figure 5b, smaller motions that are orders of magnitude below the LIS pixel size virtually disappear. The CHULL length scale distribution for propagating flashes peaks at 7 km (approximately two pixels) compared to 12 km for maximum group separation and 30 km for total branch length.

The smallest motions between groups in propagating flashes are on the scale of half of one LIS pixel. This is consistent with what is expected conceptually for the limit of LIS performance as a lightning mapping system. Without satellite motion, the smallest lateral development that LIS should be able to detect between simple (one to two pixels) groups is the case of a single pixel being illuminated in one group and then the same pixel and one of its neighbors being illuminated in a second group. In the first single-pixel group, the group centroid location is centered on the pixel. In the second two-pixel group, the centroid is located halfway between the neighboring pixels. Thus, the distance mapped between the two groups would be half a pixel. Conceptual models with smaller distances can be constructed, but they all require larger groups that differ by only one pixel at the edge flickering on and off between groups. These scenarios would not be considered "propagating" since the definition scales with footprint size, and these cases are more likely to be associated with radiative transfer than detectable lateral motion.

Branch counts for LIS flashes are shown in Figures 5c and 5d. Though Peterson, Rudlosky, et al. (2017) found extreme cases with multiple hundreds of branches, these flashes are rare as 90% of flashes contain less than 20 branches. The most frequent flash skeleton type is a linear feature that consists of a single branch. This structure describes 30% of all flashes. All of the complex flashes with extreme branch counts from

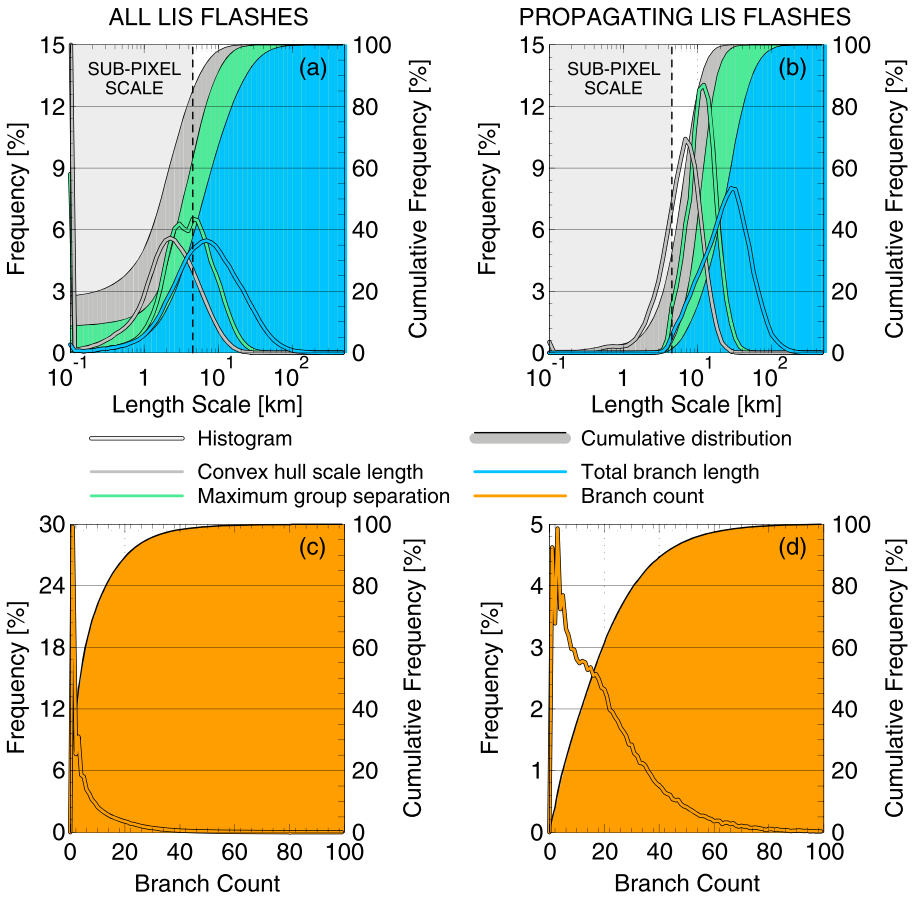

Figure 5. Histograms and cumulative distributions of (a) flash length scales for all LIS flashes, (b) flash length scales for propagating LIS flashes, (c) skeleton branch count for all LIS flashes, and (d) skeleton branch count for propagating LIS flashes. LIS = Lightning Imaging Sensor.

Peterson, Rudlosky, et al. (2017) were propagating flashes. Of these, only 4.5% contain a single branch (Figure 5d) while 4 in 10 contain 20 or more branches.

3.2. Optical Flash Orientation and Direction of Motion

Flash skeletons and CHULLs are useful for identifying the direction of lateral development and how the production of new groups relates to the existing dendritic flash structure. As discussed with Figure 3, we classify motion between groups relative to the first group centroid location and whether new development reilluminates an existing portion of the flash skeleton. Table 1 presents statistics for the composition and overall orientation of series, and the direction of development with new groups. The average flash contains seven

Table 1
The Frequency of Various Types of LIS Series- and Group-Level Motion

	Flashes			Series			Groups		
	All	Land	Ocean	All	Land	Ocean	All	Land	Ocean
Frequency	1.0×10^6	71%	29%	7.1×10^6	66%	34%	1.3×10^7	63%	37%
Mean series count	6.9	6.5	8.1	—	—	—	—	—	—
Mean group count	12	11	16	1.8	1.7	2.0	—	—	—
Outbound fraction	—	—	—	31%	29%	36%	65%	65%	65%
Extending fraction	—	—	—	33%	33%	34%	22%	22%	22%
Reilluminating fraction	—	—	—	5.2%	4.3%	6.8%	4.2%	3.7%	5.0%

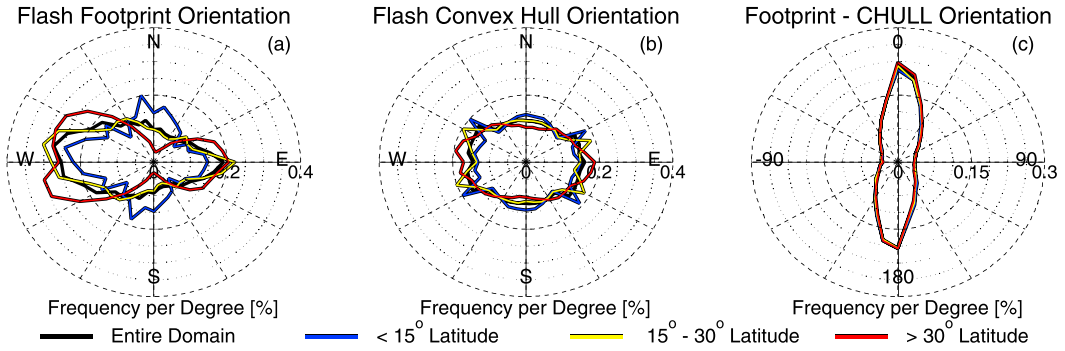

Figure 6. Polar histograms of (a) the event-based footprint orientation, (b) the group-based convex hull orientation, and (c) the difference in orientation between them for the same flash. Separate distributions are given for the entire Tropical Rainfall Measuring Mission domain, <15° latitude, 15°–30° latitude, and >30° latitude. CHULL = convex hull.

series and 12 groups, leading our one million flashes to produce 7.1 million series and 13 million groups. Seventy-one percent of our randomly selected flashes occur over land, along with their child series, and their grandchild groups. However, oceanic flashes average two additional series and four additional groups compared to their land-based counterparts. Thus, oceanic series and groups account for a larger share of all features than flashes. The average series consist of 1.8 groups due to frequent isolated LIS groups that would be defined as singleton series.

Of all series, 31% are oriented outbound, directed away from the first light location of the flash. One in three series extend the length of the flash compared to its previous state, while only 5.2% retrace an existing branch in the flash skeleton. Oceanic series are more likely to be directed outbound (36% compared to 29%) or to reilluminate an existing branch (6.8% compared to 4.3%) than flashes over land. By contrast, a much higher 65% of LIS groups are directed outbound while fewer (22%) extend their flash lengths. These fractions are invariant between land and ocean regions. This suggests that outbound-directed series consist of more groups than series that end closer to the origin than where they start.

Distributions of propagating flash orientations in geographic coordinates are shown in Figure 6. Figure 6a considers the orientations of the event-based flash footprints, Figure 6b details the orientations of group-based CHULLs, and Figure 6c computes differences in orientation between the two for the same flash. The polar distributions are based on a compass rose where flashes that are directed northward from a southern starting point are assigned a heading of 0°. Separate plots are shown for each of the following latitude belts: all latitudes (black), <15° latitude (blue), 15°–30° latitude (orange), and >30° latitude (red).

The footprints of propagating flashes are most likely to be oriented westward with a secondary maximum due east. Meridional flashes are generally less frequent than their zonal counterparts. The distributions have a strong latitude dependence, however. In the tropics <15° latitude, northward and southward flashes are each more frequent than eastward flashes, though westward flashes are still the most frequent. At the other extreme, flashes in the >30° latitude belt are frequently oriented in every direction other than north and south with the most probable orientations being southwest, northwest, and due east. The intermediate latitudes of 15° to 30° latitude are essentially an average of the tropical and subtropical regimes.

A preference in Figure 6a for westward zonal orientations at latitudes that are well known for long-lived eastward-directed mesoscale convective systems suggests that thunderstorm dynamics drives propagating flash orientation. Mature mesoscale convective systems often produce positive-polarity discharges that initiate near the convective line and then propagate rearward into the stratiform region (Carey et al., 2005; Lang et al., 2004). However, the orientations of the CHULLs that bound the skeleton of groups in the flash in Figure 6b are neither as frequently zonal nor as sensitive to latitude as the flash footprints. Subtropical groups still propagate zonally twice as often as they propagate meridionally, and the difference in orientation between the footprints and CHULLs is most frequently close to 0° or 180° in Figure 6c. Cases where the flash footprint and CHULL do not agree in orientation are likely due to the increased sensitivity of events (footprints) to radiative transfer in the cloud medium compared to groups (CHULLs), but further analysis with precipitation features and storm motion vectors will be necessary to explain these differences.

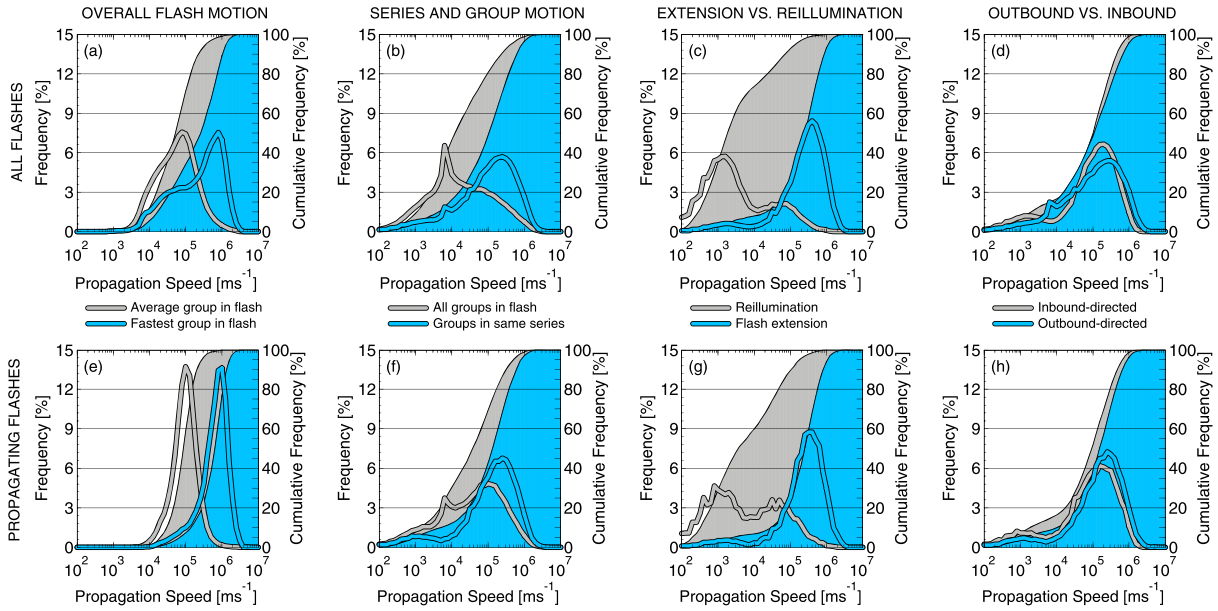

Figure 7. Histograms and cumulative distributions of the speed of Lightning Imaging Sensor (LIS) flash development for all LIS flashes (top row) and propagating LIS flashes (bottom row). (a and e) The overall average and maximum propagation speeds. (b and f) Propagation between all groups in the same flash and only groups in the same multigroup series. (c and g) The speeds of elongating and reilluminating groups. (d and h) Speeds of outbound versus inbound propagating groups.

3.3. Optical Flash Composition and Propagation Speed

With the spatial and temporal limits of LIS clustering defined in Christian et al. (2000) and herein, the question becomes what range of motion does LIS detect and how does it compare with the LMA literature. The absolute maximum speed for a simple flash that is comprised of two groups according to the clustering thresholds is 5.5 km/2 ms, or 2.75×10^6 m/s. On the other end, the speed for the smallest two-group conceptual flash from before would be 2 km/330 ms, or 6.06×10^3 m/s. Thus, we expect a range of motion that spans 3 orders of magnitude between the slowest and fastest propagating groups.

Histograms and cumulative distributions of flash, series, and group propagation speed are shown in Figure 7 for all LIS flashes (Figures 7a–7d) and propagating LIS flashes only (Figures 7e–7h). The average group development in Figure 7a peaks at 10^5 m/s, consistent with the periods of flash extension (green lines) in Figure 3. The fastest motion between connected groups in the flash skeleton is most frequently an order of magnitude greater at 10^6 m/s. Considering only propagating flashes (Figure 7e) removes many of the slower groups. The average development speed for propagating flashes ranges from 4×10^3 to 2×10^6 m/s with the fastest development speeds at ~5×10^6 m/s.

Distributions for individual groups in a series or flash are shown in Figure 7b for all flashes and Figure 7f for propagating flashes. Aside from the gray "all groups in the same flash" distributions in Figures 7b and 7f, all speeds in Figure 7 are calculated only for groups in the same series. While the average group in a LIS flash extends its branch at speeds in excess of a kilometer per second, slower groups can be noted. They can even be found in propagating flashes, adding evidence that significant lateral development in these flashes is not continuous with every subsequent group. Groups that occur in a sustained series are approximately an order of magnitude faster than general group development (Figure 7b) or twice as fast in propagating flashes (Figure 7f).

Groups that extend the length of the existing flash skeleton are some of the fastest groups observed by LIS with a peak in the distribution at 4×10^5 m/s for either all flashes (Figure 7c) or propagating flashes only (Figure 7g). Groups that reilluminate an existing part of the flash skeleton, in contrast, are frequently some of the slowest groups with a peak frequency at 10^3 m/s. Both categories of groups have a bimodal distribution with a slow peak and a fast peak, suggesting that they encompass two different types of motion. The slower peaks are likely associated with uncertainties in group centroid location that lead to subpixel-scale errors in contrast to the faster development of the physical flash.

There is also some sensitivity in development speed to the direction of motion. Figures 7d and 7h compare the distributions of inbound and outbound group motions relative to the first light centroid location. Outbound-directed flashes are slightly faster than inbound-directed flashes in both the general case (Figure 7d) and for propagating flashes only (Figure 7f). In particular, outbound groups have a higher instance of propagation speeds above 10^5 m/s, resulting in a median outbound development speed of 1.8×10^5 m/s in propagating flashes compared to a 9.1×10^4 m/s median inbound speed.

The ranges of development speeds for LIS groups, series, and flashes in Figure 7 are consistent with the speeds of leader development reviewed by Hill et al. (2011). Average propagation speeds in their Table 1 range from 8×10^4 to 1.5×10^6 m/s, while their own high-speed camera observations of leader propagation range from 2.6×10^5 to 6.2×10^5 m/s. The LMA literature reveals a similar range of propagation speeds. Ground-based propagation speed estimates depend on the type of leader involved and whether recoil processes are active (van der Velde & Montanyà, 2013). Winn et al. (2011) documented a lightning flash over the Langmuir Laboratory with an average velocity of 1.05×10^5 m/s, while van der Velde and Montanyà (2013) calculated leader speeds between 2×10^4 and 8×10^5 m/s. Rakov and Uman (1990) places the speed of stepped leaders coming to ground through virgin air at 2.0×10^5 m/s.

Instruments like LIS should be able to resolve physical lightning processes that take place at these speeds so long as they produce enough light that escapes the top of the cloud to be detected from orbit and occur over sufficiently long distances to be resolved. Stepped leader measurements from the studies spanning 76 years reviewed by Hill et al. (2011, Table 1) report interstep intervals that range from 0.2 to 200 μs and step lengths that vary between 3 and 200 m. These temporal and spatial scales correspond to 1/30,000th of a LIS frame and 1/30th of the smallest separation between subsequent propagating LIS groups. Due to the relatively long integration time of LIS, flash development may be noted in the morphologies of single LIS groups when it is not overwhelmed by scattered light, but LIS and GLM will still only be able to provide coarse snapshots of leader development that summarize many steps over multiple kilometers.

4. Conclusion

This study examines the frame-by-frame evolution of LIS flashes to quantify the scale, structure, orientation, and speed of flash optical development detected from orbit. Lightning imagers such as LIS and GLM have relatively coarse spatial (4 km for LIS, 8 km for GLM) and temporal (2 ms) resolutions compared to high-speed cameras and LMA systems but are still capable of recording the lateral development of flashes that propagate between cloud regions.

The lateral extent of a LIS flash varies according to the metric considered. Event-based quantities—such as the standard footprint area product in the science data set—are highly sensitive to radiative transfer in the cloud. Metrics that are defined using groups rather than events—such as the area or diameter of the CHULL around the group centroid locations—provide a more reasonable estimate for the scale of the underlying electrical processes responsible for the optical flash. This study tracks the development of optical LIS flashes by linking LIS groups into a skeleton image of the flash. This skeleton is used to approximate the speed and direction of new groups as they are added to the group-level structure and quantify flash complexity by counting the number of visible branches. The groups in LIS flashes, in general, are separated by a distance of 1–10 km, are organized into four or fewer branches, and propagate at speeds that range from 10^4 m/s (average for a given flash) to 10^6 m/s (fastest development in a flash). Propagating flashes, by contrast, usually contain more than 10 branches and are comprised of groups that are separated by at least one pixel and develop laterally at speeds closer to 10^5 or 10^6 m/s than to 10^4 m/s or below.

Our results demonstrate that lightning imagers such as the Optical Transient Detector, LIS, and GLM can be useful for mapping physical lightning processes. These optical sensors provide a view of flash structure that can complement ground-based measurements taken by regional LMA networks. The optical observations are shown to be potentially useful for examining processes poorly resolved in the VHF and filling data voids related to coverage gaps. The global or hemispheric domain of these systems also enables them to provide an independent assessment of lightning physics at locations that are not routinely covered by ground-based instruments such as over the open ocean.

Acknowledgments
This study was supported by NOAA grant NA14NES4320003 (Cooperative Institute for Climate and Satellites-CICS) at the University of Maryland/ESSIC, and by NASA grant NNX17AH63G. The LIS science data set is available online from the NASA Global Hydrology Resource Center DAAC, Huntsville, Alabama, USA, at https://doi.org/10.5067/LIS/LIS/DATA201. The contents of this paper are solely the opinions of the authors and do not constitute a statement of policy, decision, or position on behalf of NOAA or the U.S. government.

References

Bitzer, P. M. (2017). Global distribution and properties of continuing current in lightning. *Journal of Geophysical Research: Atmospheres*, *122*, 1033–1041. https://doi.org/10.1002/2016JD025532

Blakeslee, R. J., Christian, H. J., Stewart, M. F., Mach, D. M., Bateman, M., Walker, T. D., et al. (2014). Lightning Imaging Sensor (LIS) for the International Space Station (ISS): Mission description and science goals, *XV Int. Conf. Atmos. Electricity* (15 pp.). Norman, OK.

Boccippio, D. J., Koshak, W., Blakeslee, R., Driscoll, K., Mach, D., Buechler, D., et al. (2000). The Optical Transient Detector (OTD): Instrument characteristics and cross-sensor validation. *Journal of Atmospheric and Oceanic Technology*, *17*(4), 441–458. https://doi.org/10.1175/1520-0426(2000)017<0441:TOTDOI>2.0.CO;2

Bruning, E. C., & MacGorman, D. R. (2013). Theory and observations of controls on lightning flash size spectra. *Journal of the Atmospheric Sciences*, *70*(12), 4012–4029. https://doi.org/10.1175/JAS-D-12-0289.1

Carey, L. D., Murphy, M. J., McCormick, T. L., & Demetriades, N. W. S. (2005). Lightning location relative to storm structure in a leading-line, trailing-stratiform mesoscale convective system. *Journal of Geophysical Research*, *110*, D03105. https://doi.org/10.1029/2003JD004371

Cecil, D. J., Buechler, D. E., & Blakeslee, R. J. (2014). Gridded lightning climatology from TRMM-LIS and OTD: Dataset description. *Atmospheric Research*, *135-136*, 404–414.

Christian, H. J., Blakeslee, R. J., Goodman, S. J., & Mach, D. M. (Eds.) (2000). *Algorithm theoretical basis document (ATBD) for the Lightning Imaging Sensor (LIS)*, NASA/Marshall Space Flight Center, Alabama. Retrieved from http://eospso.gsfc.nasa.gov/atbd/listables.html, posted 1 Feb. 2000.

Coleman, L. M., Marshall, T. C., Stolzenburg, M., Hamlin, T., Krehbiel, P. R., Rison, W., & Thomas, R. J. (2003). Effects of charge and electrostatic potential on lightning propagation. *Journal of Geophysical Research*, *108*(D9), 4298. https://doi.org/10.1029/2002JD002718

Ely, B. L., Orville, R. E., Lawrence, D. C., & Hodapp, C. L. (2008). Evolution of the total lightning structure in a leading-line, trailing-stratiform mesoscale convective system over Houston, Texas. *Journal of Geophysical Research*, *113*, D08114. https://doi.org/10.1029/2007JD008445

Goodman, S. J., Blakeslee, R. J., Koshak, W. J., Mach, D., Bailey, J., Buechler, D., et al. (2013). The GOES-R geostationary lightning mapper (GLM). *Journal of the Atmospheric Research*, *125-126*, 34–49. https://doi.org/10.1016/j.atmosres.2013.01.006

Hill, J. D., Uman, M. A., & Jordan, D. M. (2011). High-speed video observations of a lightning stepped leader. *Journal of Geophysical Research*, *116*, D16117. https://doi.org/10.1029/2011JD015818

Koshak, W. J. (2010). Optical characteristics of OTD flashes and the implications for flash-type discrimination. *Journal of Atmospheric and Oceanic Technology*, *27*(11), 1822–1838. https://doi.org/10.1175/2010JTECHA1405.1

Lang, T., Pédeboy, S., Rison, W., Cerveny, R., Montanyà, J., Chauzy, S., et al. (2017). WMO world record lightning extremes: Longest reported flash distance and longest reported flash duration. *Bulletin of the American Meteorological Society*, *98*(6), 1153–1168. https://doi.org/10.1175/BAMS-D-16-0061.1

Lang, T. J., & Rutledge, S. A. (2008). Kinematic, microphysical, and electrical aspects of an asymmetric bow echo mesoscale convective system observed during STEPS. *Journal of Geophysical Research*, *113*, D08213. https://doi.org/10.1029/2006JD007709

Lang, T. J., Rutledge, S. A., & Wiens, K. C. (2004). Origins of positive cloud-to-ground lightning in the stratiform region of a mesoscale convective system. *Geophysical Research Letters*, *31*, L10105. https://doi.org/10.1029/2004GL019823

Mach, D. M., Christian, H. J., Blackeslee, R. J., Boccippio, D. J., Goodman, S. J., & Boeck, W. L. (2007). Performance assessment of the Optical Transient Detector and Lightning Imaging Sensor. *Journal of Geophysical Research*, *112*, D09210. https://doi.org/10.1029/2006JD007787

Marshall, T. C., & Rust, W. D. (1993). Two types of vertical electrical structures in stratiform precipitation regions of mesoscale convective systems. *Bulletin of the American Meteorological Society*, *74*(11), 2159–2170. https://doi.org/10.1175/1520-0477(1993)074<2159:TTOVES>2.0.CO;2

Marshall, T. C., Stolzenburg, M., Krehbiel, P. R., Lund, N. R., & Maggio, C. R. (2009). Electrical evolution during the decay stage of New Mexico thunderstorms. *Journal of Geophysical Research*, *114*, D02209. https://doi.org/10.1029/2008JD010637

Peterson, M. J., Deierling, W., Liu, C., Mach, D., & Kalb, C. (2017). The properties of optical lightning flashes and the clouds they illuminate. *Journal of Geophysical Research: Atmospheres*, *122*, 423–442. https://doi.org/10.1002/2016JD025312

Peterson, M. J., & Liu, C. (2011). Global statistics of lightning in anvil and stratiform regions over the tropics and subtropics observed by TRMM. *Journal of Geophysical Research*, *116*, D23201. https://doi.org/10.1029/2011JD015908

Peterson, M. J., & Liu, C. (2013). Characteristics of lightning flashes with exceptional illuminated areas, durations, and optical powers and surrounding storm properties in the tropics and inner subtropics. *Journal of Geophysical Research*, *118*, 11,727–11,740. https://doi.org/10.1002/jgrd.50715

Peterson, M. J., Rudlosky, S., & Deierling, W. (2017). The evolution and structure of extreme optical lightning flashes. *Journal of Geophysical Research: Atmospheres*, *122*, 13,370–13,386. https://doi.org/10.1002/2017JD026855

Rakov, V. A., & Uman, M. A. (1990). Waveforms of first and subsequent leaders in negative lightning flashes. *Journal of Geophysical Research*, *95*(D10), 16,561–16,577. https://doi.org/10.1029/JD095iD10p16561

Rison, W., Thomas, R. J., Krehbiel, P. R., Hamlin, T., & Harlin, J. (1999). A GPS-based three-dimensional lightning mapping system: Initial observations in central New Mexico. *Geophysical Research Letters*, *26*(23), 3573–3576. https://doi.org/10.1029/1999GL010856

Rudlosky, S. D., Peterson, M. J., & Kahn, D. T. (2017). GLD360 performance relative to TRMM LIS. *Journal of Atmospheric and Oceanic Technology*, *34*(6), 1307–1322. https://doi.org/10.1175/JTECH-D-16-0243.1

Rutledge, S. A., & MacGorman, D. R. (1988). Cloud-to-ground lightning activity in the 10-11 June 1985 mesoscale convective system observed during the Oklahoma-Kansas PRESTORM project. *Monthly Weather Review*, *116*(7), 1393–1408. https://doi.org/10.1175/1520-0493(1988)116<1393:CTGLAI>2.0.CO;2

Schonland, B. F. J., Malan, D. J., & Collens, H. (1935). Progressive lightning II. *Proceedings of the Royal Society of London, Series A*, *152*(877), 595–625. https://doi.org/10.1098/rspa.1935.0210

Schuur, T. J., & Rutledge, S. A. (2000). Electrification of stratiform regions in mesoscale convective systems. Part II: Two-dimensional numerical model simulations of a symmetric MCS. *Journal of the Atmospheric Sciences*, *57*(13), 1983–2006. https://doi.org/10.1175/1520-0469(2000)057<1983:EOSRIM>2.0.CO;2

Stolzenburg, M., Marshall, T. C., Rust, W. D., & Smull, B. F. (1994). Horizontal distribution of electrical and meteorological conditions across the stratiform region of a mesoscale convective system. *Monthly Weather Review*, *122*(8), 1777–1797. https://doi.org/10.1175/1520-0493(1994)122<1777:HDOEAM>2.0.CO;2

Thomas, R. J., Krehbiel, P. R., Rison, W., Hamlin, T., Boccippio, D. J., Goodman, S. J., & Christian, H. J. (2000). Comparison of ground-based 3-dimensional lightning mapping observations with satellite-based LIS observations in Oklahoma. *Geophysical Research Letters*, *27*(12), 1703–1706. https://doi.org/10.1029/1999GL010845

Thomson, L. W., & Krider, E. P. (1982). The effects of clouds on the light produced by lightning. *Journal of the Atmospheric Sciences*, *39*(9), 2051–2065. https://doi.org/10.1175/15200469(1982)039<2051:TEOCOT>2.0.CO;2

Uman, M. A. (1987). *The lightning discharge*. New York: Elsevier.

van der Velde, O. A., & Montanyà, J. (2013). Asymmetries in bidirectional leader development of lightning flashes. *Journal of Geophysical Research: Atmospheres*, *118*, 13,504–13,519. https://doi.org/10.1002/2013JD020257

Williams, E. R., Weber, M. E., & Orville, R. E. (1989). The relationship between lightning type and convective state of thunderclouds. *Journal of Geophysical Research*, *94*(D11), 13,213–13,220. https://doi.org/10.1029/JD094iD11p13213

Winn, W. P., Aulich, G. D., Hunyady, S. J., Eack, K. B., Edens, H. E., Krehbiel, P. R., et al. (2011). Lightning leader stepping, K changes, and other observations near an intracloud flash. *Journal of Geophysical Research*, *116*, D23115. https://doi.org/10.1029/2011JD015998